TENSILE PROPERTIES OF EARLYWOOD AND LATEWOOD FROM LOBLOLLY PINE (*PINUS TAEDA*) USING DIGITAL IMAGE CORRELATION

Gi Young Jeong
Graduate Research Assistant
Department of Wood Science and Forest Products
Virginia Polytechnic Institute and State University
Brooks Forest Products Center
1650 Ramble Road
Blacksburg, VA 24061-0503

Audrey Zink-Sharp†
Professor
Department of Wood Science and Forest Products
Virginia Polytechnic Institute and State University
230 Cheatham Hall
Blacksburg, VA 24061-0323

*Daniel P. Hindman**†
Assistant Professor
Department of Wood Science and Forest Products
Virginia Polytechnic Institute and State University
Brooks Forest Products Center
1650 Ramble Road
Blacksburg, VA 24061-0503

(Received August 2008)

Abstract. The goal of this research was to measure the elastic properties and strength of earlywood and latewood from two growth-ring positions of loblolly pine. Because of the small specimen size, a contactless strain measurement was applied using a microscope with an appropriate field of view. The tensile properties of the earlywood and latewood were calculated from load data from a Minimat tester coupled with elastic strain data from a digital image correlation technique. Incremental loading was applied until specimen failure occurred. Elastic modulus, Poisson ratio, and strength generally increased as the growth-ring numbers increased, except for the strength of latewood that slightly decreased. Elastic properties and strength were significantly different for different growth-ring positions and intraring layers. The elastic modulus for earlywood and latewood were best fitted by Weibull distributions regardless of growth-ring positions, whereas Poisson ratios were best fitted by Weibull distributions for earlywood 1 – 10 and latewood 11 – 20 groups, and gamma distributions for earlywood 11 – 20 and latewood 1 – 10 groups. Strain distribution analysis showed nonuniform strain distributions for the four groups and also showed more resistance to load for earlywood and latewood from a higher growth-ring position.

Keywords: Earlywood, latewood, digital image correlation (DIC), modulus of elasticity (MOE), ultimate tensile strength (UTS), Poisson ratio.

INTRODUCTION

A large portion of the wood resources for strand-based composites are supplied from plantation-grown trees. These trees are harvested on a short-term rotation, resulting in small-diameter logs and a high proportion of juvenile wood (Larson et al 2001). This situation has placed pressure on the industry to use wood resources more efficiently for strand-based composite production. Although there is more interest in the efficient use of wood resources, there is lack of

* Corresponding author: dhindman@vt.edu
† SWST member

knowledge on the mechanical behavior of earlywood and latewood layers of loblolly pine (*Pinus taeda* L.). Different morphological and chemical variations of wood cells for earlywood and latewood produce different physical properties. Comprehensive knowledge of certain physical properties of earlywood and latewood, including cell length, chemical composition, microfibril angle, and specific gravity, is available from previous work (Taylor and Moore 1981; Bendtsen and Senft 1986; Larson et al 2001; Yeh et al 2006).

Indeed, it is hardly surprising that previous researchers have measured different mechanical properties between earlywood and latewood. There is little information about the effect of the growth-ring numbers on the mechanical properties of earlywood and latewood. From pith to bark, there are many changes in anatomical structure, including smaller microfibril angles and larger cell diameters (Taylor and Moore 1981; Bendtsen and Senft 1986; Larson et al 2001). These changes in earlywood and latewood properties may lead to fundamental changes in wood materials, which could affect wood composite production. Therefore, measurement of earlywood and latewood from different growth-ring positions can help maximize resource use.

However, elastic properties are difficult to measure for earlywood and latewood bands as a result of the small specimen sizes. Because it is difficult to use an extensometer or strain gauge mounted to the surface of the earlywood and latewood without interference of strain measurement, noncontact methods are required to measure the elastic strain to calculate the elastic modulus. Digital image correlation (DIC) is one of the alternative options for this case because this technique uses images of the surface of test specimens acquired during testing. Although the DIC is well developed and widely used to measure the strain distribution of materials qualitatively, there is lack of research on measuring elastic strain for wood material quantitatively. To apply DIC to measure the elastic strain, a complex testing setup and many calibrations are needed to have accurate results. In this study, earlywood and latewood properties from two different growth-ring positions were measured using DIC. Understanding earlywood and latewood properties from different growth-ring positions will permit improved characterization of the constitutive behavior of wood strands and provide more detailed characterization of the mechanical behavior.

LITERATURE REVIEW

Previous Measurement of Intraring Properties

Previous studies have used different test methods to measure elastic properties of earlywood and latewood from different wood species. Table 1 includes previous work showing differences in mechanical properties of earlywood and latewood from loblolly pine (*Pinus taeda*). Although Groom et al (2002) and Mott et al (2002) measured the properties of a single fiber, Kretschmann et al (2006) and Hindman and Lee (2007) measured the properties of small specimens of earlywood and latewood from loblolly pine. The presented values are the longitudinal elastic moduli of earlywood and latewood and the longitudinal strength of earlywood and latewood.

Groom et al (2002) measured the modulus of elasticity (MOE) and ultimate tensile strength (UTS) of latewood tracheids of loblolly pine in different growth-ring positions and tree heights. The MOE of latewood increased from 6.55 – 27.5 GPa as the ring number increased from pith to mature areas. The strength of latewood increased from 410 – 1422 MPa as the growth-ring position moved from pith to the mature portion.

Mott et al (2002) studied mechanical properties of earlywood of loblolly pine using a tensile tester with loading speed of 80 μm/min. The MOE and UTS of juvenile earlywood tracheids were 11.7 GPa and 496 MPa, whereas those of mature earlywood fibers were 17.2 GPa and 648 MPa, respectively. Microfibril angle (MFA) for juvenile wood was 25 – 30° and MFA for mature wood was 5 – 10°. Based

Table 1. *Previous works on single-fiber (Groom et al 2002; Mott et al 2002) and small specimen test (Kretschmann et al 2006; Hindman and Lee 2007) showing test conditions and results.*

Researchers	Species	Loading speed (μm/min)	Earlywood E_L (GPa)	Earlywood σ_L (MPa)	Latewood E_L (GPa)	Latewood σ_L (MPa)
Groom et al (2002)	Loblolly pine (*Pinus taeda*)	80	N/A	N/A	6.55 – 27.5	410 – 1422
Mott et al (2002)	Loblolly pine (*Pinus taeda*)	80	14.8	604	N/A	N/A
Kretschmann et al (2006)	Loblolly pine (*Pinus taeda*)	N/A[a]	3.5[b] 5.1[c]	N/A	8.1[b] 13.0[c]	N/A
Hindman and Lee (2007)	Loblolly pine (*Pinus taeda*)	127	2.71	27.5	6.38	48.8

[a] Not applicable.
[b] Earlywood and latewood at a height of approximately 1.5 m.
[c] Earlywood and latewood at a height of approximately 6 m.
E_L, longitudinal elastic moduli; σ_L, longitudinal strength.

on these results, Mott et al (2002) concluded that the MOE and UTS were dependent on MFA.

Burgert et al (2003) combined video extensometry with a microtensile tester to determine MOE and UTS of 10 GPa and 530 MPa, respectively, for mature spruce fiber in a transition zone between earlywood and latewood. Displacement was measured using video extensometry instead of cross-head movement for specimen deformation. This method provided a more reliable MOE value.

Kretschmann et al (2006) used a broadband viscoelastic spectroscopy instrument (BVS) to measure MOE and shear modulus of earlywood and latewood of six loblolly pine trees. Samples $1 \times 1 \times 30$ mm were obtained from different growth-ring numbers and different heights. MOE of earlywood increased from 3.5 – 5.1 GPa as the height increased from 1.5 – 6 m; MOE of latewood increased from 8.1 – 13.0 GPa as the height increased from 1.5 – 6 m.

Hindman and Lee (2007) measured the MOE and UTS of earlywood and latewood bands from loblolly pine using a tensile tester with a loading rate of 127 μm/min. Earlywood samples of $0.66 \times 4.58 \times 60$ mm and latewood samples of $0.66 \times 3.3 \times 60$ mm were used. The MOE and UTS from earlywood were 2.71 GPa and 27.5 MPa, respectively, whereas those from latewood were 6.38 GPa and 48.8 MPa.

Previous work to characterize the wood properties of earlywood and latewood has used the cross-head movement as deformation of the specimen (Groom et al 2002; Mott et al 2002; Hindman and Lee 2007). These measurements assumed no slippage in the grips. Also, uniform elastic strain through the entire span of the specimen was assumed. From the result of Burgert et al (2003), refinement of measurement on displacement of the specimen can be found. As a result of the size of the specimen used for testing, an accurate measurement of elastic strain is a key component to calculate MOE. Therefore, the elastic strain of earlywood and latewood should be determined from measurement of the center section apart from the edge to avoid edge effect. One method for measuring elastic strain in the center of a specimen is the DIC method, which has the advantage of being able to track the change in position of a point in the field under study.

Digital Image Correlation for Strain Measurement

DIC was developed to resolve the displacement on the surface of a specimen by correlating subimages of a sequence of images, one before loading and several images during loading. Deformation of the material can be achieved by tracking the displacement of markers on the sample surface. The advantage of DIC is that it

can avoid overestimated strain from slippage of the clamp and the effect of the low stiffness of the test specimen. Figure 1 demonstrates the general scheme of tracking the displacement of the window on the sequence of images. The first step is to locate the interest point, P, in the image of the reference configuration before loading by virtually generating a grid. The virtual fixed grid on the image has information of the exact location of the point, P. After loading, the change in the location of Point P is tracked by image correlation using a pattern matching technique. Eight subsets of pixels surrounding Point P in the reference image, called a template or window, are matched with similarly sized subsets of pixels within a search window determined by the maximum expected interimage displacement without a marker. Tracking of a subimage can be achieved by maximizing the crosscorrelation coefficient between gray value patterns of two images (Sun et al 2005).

Many previous researchers have applied DIC to wood and wood-based materials. After the DIC technique was introduced to measure the strain distribution of wood and paper material by Choi et al (1991), there was a body of DIC applications to wood material (Zink et al 1995, 1997; Mott et al 1996; Stelmokas et al 1997; Muszynski et al 2000; Murata and Masuda 2001; Danvind 2002; Samarasinghe and Kulasiri 2004; Penneru et al 2005; Serrano and Enquist 2005; Ljungdahl et al 2006; Keunecke and Niemz 2008). Although the main application of DIC to wood material was to measure the strain distribution, most DIC applications were not applied to quantify the average strain. Although the strain distribution showed qualitative information, the information could not validate and compare with quantitative properties from other test methods. Therefore, a novel procedure was required to quantify tensile properties of earlywood and latewood.

The objective of this study is to measure MOE, Poisson ratio, and UTS of loblolly pine earlywood and latewood from different growth-ring positions using DIC. A specific guideline for using DIC to measure elastic properties of earlywood and latewood from growth-ring numbers 1 – 10 and growth-ring numbers 11 – 20 was developed. Elastic properties of the earlywood and latewood were calculated from load data from the Minimat tester (Rheometric Scientific, currently T.A. Instruments–Waters LLC, New Castle, DE) coupled with elastic strain data from a DIC technique. Strain distribution within the earlywood and latewood samples was also observed.

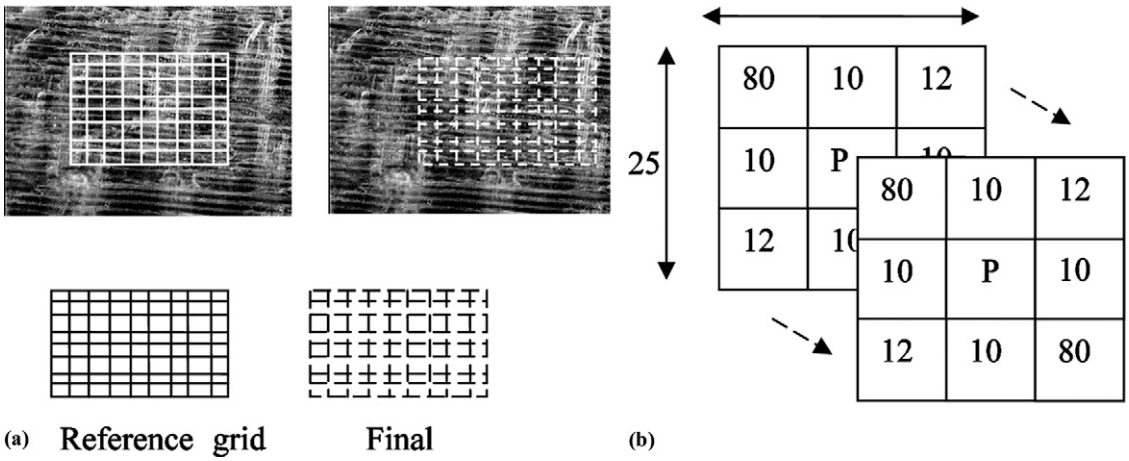

Figure 1. Crosscorrelation techniques for digital image correlation: (a) a sequence of images showing the change of grid positions; (b) crosscorrelation matching technique.

MATERIALS AND METHODS

Material Preparation

A 25-yr-old loblolly pine from Reynolds Homestead Research Center in Patrick County, VA, was chosen for this study. Four wood disks were cut approximately 0.6 m high from the ground. Wood blocks 13.9 × 13.3 × 5.08 cm were taken from growth-ring numbers 1 – 10 and 11 – 20 from the pith. As a result of the method of strand generation, finer gradations into discrete growth rings were not obtained. All wood blocks were submerged in water and a vacuum was applied to minimize cutting damage. Strands were processed from a flaker located at the Brooks Forest Products Center. Earlywood and latewood specimens were prepared from aligned strands using a razor knife and a metal ruler. Aligned strands were cut to 55 × 10 × 0.5 mm of earlywood and latewood from growth-ring numbers 1 – 10 from the pith and the same size of earlywood and latewood from growth-ring numbers 11 – 20 from pith. Four specimen groups were obtained from the same disk with a sample size of 50 for each group. Figure 2 shows the segmented earlywood and latewood bands from a strand. After extracting the earlywood and latewood separately, both earlywood and latewood bands were carefully placed into reclosable bags. Strands were kept in an environmental chamber to normalize the MC at 6% for 1 mo.

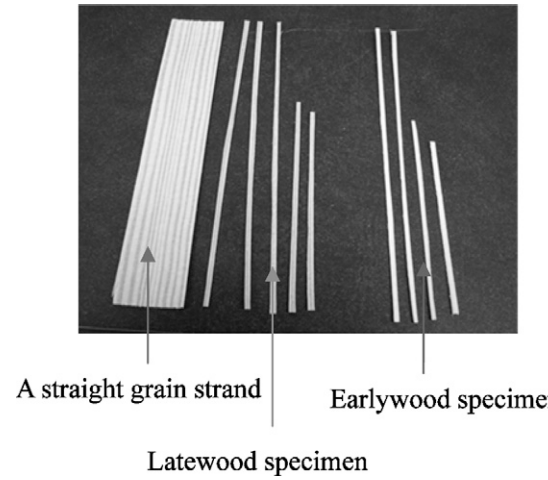

Figure 2. Segmentation of earlywood and latewood specimensfrom a strand.

Test Setup

Specimens were tested using a Minimat tester and a Zeiss microscope with a 10× ocular and 2.5× objective lens. Minimat test frame contained a 200 N load cell and computer-controlled displacement with cross-head travel range of 100 mm and sensitivity of 0.15 m. The Zeiss microscope had a DAGE MTI 72 CCD camera attached to capture the surface of the test specimen. Resolution of the camera was 768 × 493 pixels. Spatial size of the image pixel was calculated using a stage micrometer (100 units in 3 mm) correlated with pixel size of the image in the field of view on the specimen. The spatial resolution of the camera was 11 × 13 μm/pixel. Field of view was calculated to be 4.20 mm (horizontal) × 3.22 mm (vertical). Resolution of the image was 632 × 480 pixels. Pixel size in the spatial area was determined to be 6.64 × 6.71 μm. However, subpixels were set to 1/1000 pixel to match the displacement of the sequence of images using crosscorrelation and cubic interpolation. Therefore, the pixel resolution can detect a minimum length change of 6.64 × 6.71 nm.

The Minimat test frame was mounted on a newly designed stage, which has a fine level adjustment and two side bars with screws to hold the Minimat tightly (Fig 3). The designed stage has two legs on the left side to minimize vibration during testing. Specimens were gripped at both ends using metal jaws. Span length between the grips was 40 mm. Specimens were loaded at a rate of 0.126 mm/min. A preload of 1 N was applied to stabilize the specimen and to adjust the focus of the lens. From preliminary testing, this preload represents less than 2% of the failure load and is well within the elastic range. After adjusting the focus distance, tensile testing continued until the specimen failed. Incremental loading was applied to prevent the capture of distorted images for strain determination. Capture of images during loading can cause greater

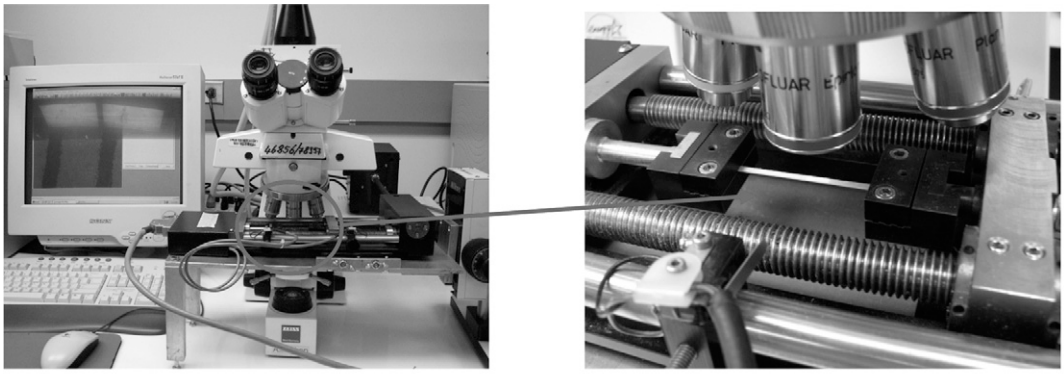

(a) (b)

Figure 3. Microtensile test setup for applying tensile load and capturing surface images of earlywood and latewood: (a) microtensile test setup with a Zeiss microscope; (b) a tensile specimen at 2.5× magnification.

than true strain (Mott et al 1996). Test was paused for 8 s while each image was captured. To have clear contrast for image correlation, a speckle pattern was generated on the surface of the specimen using carbon-black particles and a paint brush. Images were taken every 20 s for up to 300 s. To minimize the influence of light other than a fiberoptic lamp, all testing was conducted at night with no room light. All input devices, including the mouse and keyboard, were placed on a different table to avoid creating vibration while conducting the testing. To analyze the effect of the pause time on relaxation of specimen, images were taken every 2 s up to 120 s. The results showed only 1% change in strain compared with the change of strain value for calculating elastic modulus. Therefore, the effect of the 8 s pause time on the strain variation can be ignored.

Strain Measurement Using Digital Image Correlation

Strain was measured from the sequence of specimen images within the elastic range under tension loading using DIC software coded by Eberl et al (2006). Different window sizes of 200, 100, 50, 25, 15, and 10 pixels were used to check convergence of the strain value. A 25 pixel window size was chosen for the actual image correlation for strain measurement. While the image correlation was running, the change of the tracking point was also examined by looking at the sequence of images. The out-of-range correlation samples were eliminated by visual inspection.

To detect small strain, the conventional DIC considers a homogeneous deformation on the surface of the specimens and uses subpixel correlation. A subset-based correlation compares a subset of pixel intensities from the undeformed image with a subset of pixel intensities after loading using interpolation. If the material is not homogeneous, higher-order interpolation is required, whereas homogeneous materials only require zero- or first-order interpolation to approximate the variation of the displacement field (Jin and Bruck 2005). In this study, a cubic spline interpolation scheme was used to represent the inhomogeneous displacement field of wood. Image acquisition and deflection rate were synchronized to evaluate the elastic modulus. A virtual reference grid was generated on the first image before the load was applied. The grid point was tracked by correlated gray scale of the region around the reference point as the image goes from the first to the last.

Specific Gravity Measurement

Specific gravity was obtained from untested samples of the same population measured

according to ASTM D 2395 (ASTM 2004a). To minimize the influence of the environment of room humidity and temperature before testing, all samples were kept in the recloseable bag and handled by forceps when the specimens were mounted on the balance. The balance has a sensitivity of ± 10 μg. Volume of specimens was measured using a microcaliper having a sensitivity of ± 0.001 mm. After measuring the specimen weight, all samples were kept in petri dishes and covered by a recloseable bag. To measure the oven-dry weight, the petri dishes were placed in the oven for 24 h. Specific gravity was measured based on the oven-dry weight and volume at the same condition as during mechanical testing.

RESULTS AND DISCUSSION

Experimental Results

Table 2 provides a summary of the test results from the four sample groups. Specific gravity increased as growth-ring number increased. The latewood-specific gravity from growth-ring numbers 1 – 10 and from growth-ring numbers 11 – 20 had 74 and 26% higher specific gravity than the earlywood from growth-ring numbers 1 – 10 and growth numbers 11 – 20. However, for latewood 1 – 10 and latewood 11 – 20, the specific gravity was slightly decreased from 0.54 – 0.53, respectively.

Latewood 11 – 20 had the highest MOE of 5.09 GPa with coefficient of variance (COV) of 36%, whereas earlywood 1 – 10 had the lowest MOE of 1.92 GPa with COV of 31%. Compared with the MOE of earlywood 1 – 10 and earlywood 11 – 20, the MOE of latewood 1 – 10 and latewood 11 – 20 was 1.79 and 2.05 times higher, respectively. Compared with the MOE of earlywood 1 – 10 and latewood 1 – 10, the MOE of earlywood 11 – 20 and latewood 11 – 20 was 1.29 and 1.48 times higher, respectively.

Latewood 1 – 10 had the highest UTS of 34.21 MPa with COV of 37%, whereas earlywood 1 – 10 had the lowest UTS of 18.69 MPa with COV of 35%. Compared with the UTS of earlywood 1 – 10 and earlywood 11 – 20, the UTS of latewood 1 – 10 and latewood 11 – 20 was 1.83 and 1.33 times higher, respectively. Compared with the UTS of earlywood 1 – 10 and latewood 1 – 10, the UTS of earlywood 11 – 20 and latewood 11 – 20 was 1.33 times higher and 0.97 times lower, respectively.

Latewood 11 – 20 had the highest Poisson ratio of 0.8 with COV of 54%, whereas the lowest Poisson ratio found was 0.49 with COV of 53% and with COV of 54% from earlywood 1 – 10 and earlywood 11 – 20. Compared with the Poisson ratio of earlywood 1 – 10 and earlywood 11 – 20, the Poisson ratio of latewood 1 – 10 and latewood 11 – 20 was 1.20 and 1.63 times higher, respectively. Compared with the Poisson ratio of earlywood 1 – 10 and latewood 1 – 10, the Poisson ratio of earlywood 11 – 20 and latewood 11 – 20 was 1.0 times and 1.35 times higher, respectively.

Except for UTS of latewood 1 – 10 and latewood 11 – 20, the general trend was that as the growth-ring number increased, the UTS, MOE, and Poisson ratios also increased. Although specific gravity was highly correlated with UTS from earlywood and latewood, specific gravity was weakly correlated with MOE from

Table 2. *Physical properties and mechanical properties of earlywood and latewood from growth rings 1 – 10 and growth rings 11 – 20.*

	SG		MOE (GPa)		UTS (MPa)		Poisson ratio	
Test groups	AVE	COV	AVE	COV	AVE	COV	AVE	COV
Earlywood 1 – 10	0.31	13%	1.92	31%	18.69	35%	0.49	53%
Latewood 1 – 10	0.54	8%	3.44	31%	34.21	37%	0.59	48%
Earlywood 11 – 20	0.42	7%	2.48	29%	25.01	29%	0.49	54%
Latewood 11 – 20	0.53	7%	5.09	36%	33.47	27%	0.80	54%

SG, specific gravity; MOE, modulus of elasticity; UTS, ultimate tensile strength; AVE, average; COV, coefficient of variance.

latewood. Weak correlation between specific gravity and MOE of earlywood and latewood was also found by Cramer et al (2005) and Kretschmann et al (2006). Less variation of physical and mechanical properties of earlywood and latewood was found as the growth-ring numbers increased from 1 – 10 to 11 – 20. The decrease in variation of earlywood and latewood from higher growth-ring numbers may be the result of more mature earlywood and latewood, which contains a lower MFA with microfibrils more closely oriented in the direction of the longitudinal axis. Previous results also found that as growth-ring numbers increased, MFA decreased (Groom et al 2002; Kretschmann et al 2006). The lowered reinforcement in the off-axis direction of the loading direction resulting from the lower MFA in a higher growth-ring position could have resulted in a smaller strain imposed in the longitudinal direction, which may result in a higher Poisson ratio if the transverse strain behavior remains unchanged.

Figure 4 shows the relationship between tree height and average MOE from earlywood and latewood from the same species. The average MOE data at growth-ring numbers 1 – 20 from 0.6 m tree height were used from current study. The average MOE data at growth-ring numbers 3, 6, 12, and 18 from 1.5 and 6 m height were obtained from a previous study (Kretschmann et al 2006). The correlation between MOE of earlywood and height, between MOE of latewood and height, and among the MOE, ratio of latewood to earlywood, and height showed a strong positive linear relation presenting R^2 of 0.996, 0.995, and 0.931, respectively. From the MOE ratio of latewood to earlywood as a function of height, the MOE of latewood increased more than that of earlywood. It can be speculated that in the lower height of the tree, earlywood and latewood fiber structures are physiologically adapted to support compression by tree mass and gravity with higher MFA, thicker cell wall diameter, larger cell dimension, and shorter fiber lengths, whereas in the upper height of tree, earlywood and latewood fiber structures are adapted to support tension by wind and growth stress with lower MFA, thinner cell wall diameter, smaller cell dimension, and longer fiber length (Groom et al 2002; Mott et al 2002; Burdon et al 2004; Xu et al 2004; Cramer et al 2005; Kretschmann et al 2006; Yeh et al 2006). These speculations on the anatomical structure adaptations of earlywood and latewood provide relative comparisons for the earlywood and latewood material behavior from three different heights. More data and analysis would be required to develop the relationship between earlywood and latewood properties and tree height.

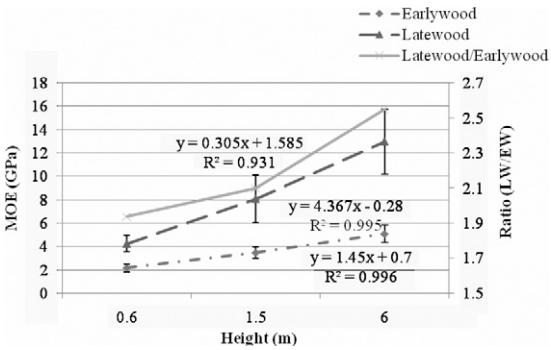

Figure 4. Earlywood modulus of elasticity (MOE), latewood MOE, and ratio of latewood MOE to earlywood MOE as a function of tree heights from current test results including data at 0.6 m height and a previous study by Kretschmann et al (2006) including data at 1.5 and 6 m height.

Table 3 shows the summary of the two-way analysis of variance results considering factors of growth-ring and intraring positions on the MOE, UTS, and Poisson ratio from the sample groups. Alpha of 0.05 was used as a significant difference. Although there were many other interaction results between growth-ring numbers and intraring layers, only the physically meaningful comparisons are shown in Table 3. Overall comparison between growth-ring numbers 1 – 10 and growth-ring numbers 11 – 20 shows significant differences in MOE, UTS, and Poisson ratio. Overall, comparison between earlywood and latewood also showed significant differences in MOE, UTS, and Poisson ratio. When looking at the detailed comparison of

Table 3. *Statistical comparison of the tensile properties for earlywood and latewood from two different growth ring positions: growth ring numbers 1 – 10 and growth ring numbers 11 – 20 ($\alpha = 0.05$).*

Variable A	Variable B	*p* value for MOE	*p* value for UTS	*p* value for Poisson ratio
Growth ring position 1 – 10	Growth ring position 11 – 20	<0.0001	0.006	0.030
Earlywood	Latewood	<0.0001	<0.0001	<0.0001
Earlywood 1 – 10	Earlywood 11 – 20	0.006	0.0003	0.440
Earlywood 1 – 10	Latewood 1 – 10	<0.0001	<0.0001	0.017
Earlywood 11 – 20	Latewood 11 – 20	<0.0001	<0.0001	<0.0001
Latewood 1 – 10	Latewood 11 – 20	<0.0001	0.831	0.028

MOE, modulus of elasticity; UTS, ultimate tensile strength.

interaction between growth-ring numbers and intraring layers, all MOE comparisons showed significant differences, which agreed with the results from Table 2. For the UTS, only the comparison between latewood 1–10 and latewood 11 – 20 was not significantly different, which agreed with results from Table 2 showing that 34.21 MPa for latewood 1–10 with COV of 31% and 33.47 MPa for latewood 11 – 20 with COV of 36%. The difference of specific gravity between latewood 1–10 and latewood 11 – 20 was only 1.8%. For Poisson ratio, all comparisons showed a significant difference except for the case between earlywood 1 – 10 and earlywood 11 – 20, which also agrees with the results from Table 2.

Table 4 shows the distribution fitting for MOE, UTS, and Poisson ratio from four groups. The alpha value of 0.05 was used to find the best fitting curve for the MOE, UTS, and Poisson ratio from normal, log normal, Weibull, and gamma distribution using SAS 9.1 (SAS Institute Inc. 2004). The distribution fitting was examined by Kolmogorov-Smimov (K-S) and χ^2 test. Visual inspection was also conducted for estimating the best fitting curve. Based on the *p* values from K-S, χ^2 test, and visual inspection, the Weibull distributions were chosen as the best fitting curve with the three estimated parameters. The best fitting curves for UTS of earlywood 1 – 10 and latewood 1 – 10 were Weibull distribution, whereas earlywood 11 – 20 and latewood 11 – 20 groups were log normal. However, for the earlywood 11 – 20 group, χ^2 test was below a *p* value of 0.05. For the Poisson ratio, earlywood 1 – 10 and latewood 11 – 20 groups were fitted best with the Weibull distribution, whereas the latewood 1 – 10 and earlywood 11 – 20 groups followed with the gamma distribution. Analytical distribution of mechanical properties for earlywood and latewood from different growth-ring numbers could be used for numerical modeling.

Strain Distribution of Earlywood and Latewood from Growth-Ring Numbers 1 – 10 and 11 – 20

Representative strain distributions of one sample from each test group are shown in Figs 5 and 6. The strain distribution in x is the direction parallel to the load direction, whereas strain distribution in the y direction is the direction perpendicular to the loading direction. To compare the strain distribution for earlywood and latewood from different growth-ring positions at a similar stress level, a sequence from images correlation is shown; the seventh image for earlywood 1 – 10, the fourth image for latewood 1 – 10, the sixth image for earlywood 11 – 20, and the second image for latewood 11 – 20, which were under elastic range. Typically, failure of earlywood and latewood occurred at least after the 10th image for all groups.

Figure 5 shows the strain distribution of sample number 45 from earlywood 1 – 10 and sample number 50 from latewood 1 – 10. The strain distributions in x and y directions for latewood 1 – 10 showed more resistance under similar stress level, showing that approximately one magnitude smaller strain occurred. The latewood 1 – 10 strain distribution showed higher

Table 4. *Distribution fitting for tensile properties of earlywood and latewood from growth ring numbers 1 – 10 and growth ring numbers 11 – 20 (α = 0.05).*

	Normal		Lognormal		Weibull		Gamma	
Test groups	K-S	χ^2	K-S	χ^2	K-S	χ^2	K-S	χ^2
MOE								
Earlywood 1 – 10	0.14	0.32	0.25	0.26	0.11	0.31	0.09	0.30
Latewood 1 – 10	0.15	0.29	0.25	0.26	0.25	0.51	0.25	0.36
Earlywood 11 – 20	0.15	0.15	0.50	0.05	0.5	0.08	0.02	0.08
Latewood 11 – 20	0.06	0.28	0.5	0.71	0.5	0.85	0.5	0.79
UTS								
Earlywood 1 – 10	0.15	0.23	0.25	0.17	0.5	0.22	0.25	0.22
Latewood 1 – 10	0.13	0.14	0.23	0.75	0.14	0.40	0.25	0.67
Earlywood 11 – 20	0.08	0.001	0.25	0.01	NA	0.001	0.25	0.004
Latewood 11 – 20	0.15	0.07	0.23	0.05	0.25	0.04	N/A	N/A
Poisson ratio								
Earlywood 1 – 10	0.15	0.03	0.04	N/A	0.5	0.50	0.25	0.59
Latewood 1 – 10	0.02	0.001	0.04	0.17	0.06	0.05	0.25	0.17
Earlywood 11 – 20	0.01	0.001	0.03	0.13	0.007	0.04	0.06	0.09
Latewood 11 – 20	0.01	0.001	0.25	0.11	0.25	0.25	0.13	0.04

MOE, modulus of elasticity; K-S, Kolmogorov-Smimov; UTS, ultimate tensile strength; N/A, not applicable.

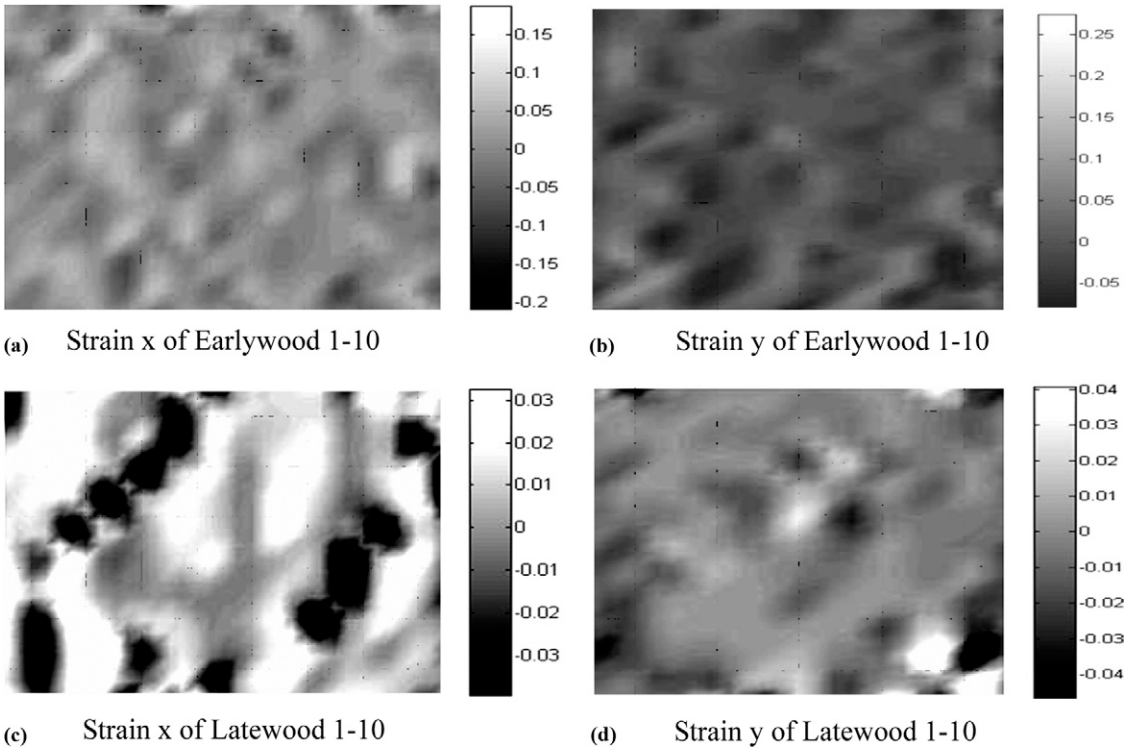

Figure 5. Strain distribution of earlywood and latewood from growth-ring numbers 1 – 10 (specimen number 45 under 19.6 MPa, specimen number 50 under 21.9 MPa).

proportions of negative strain distributions in the x direction to the positive strain by applied load and higher proportions of negative strain distributions in the y direction to the negative strain by applied load. As a result of the strain distribution of earlywood and latewood, latewood 1 – 10 had higher MOE and Poisson ratio found in Table 2.

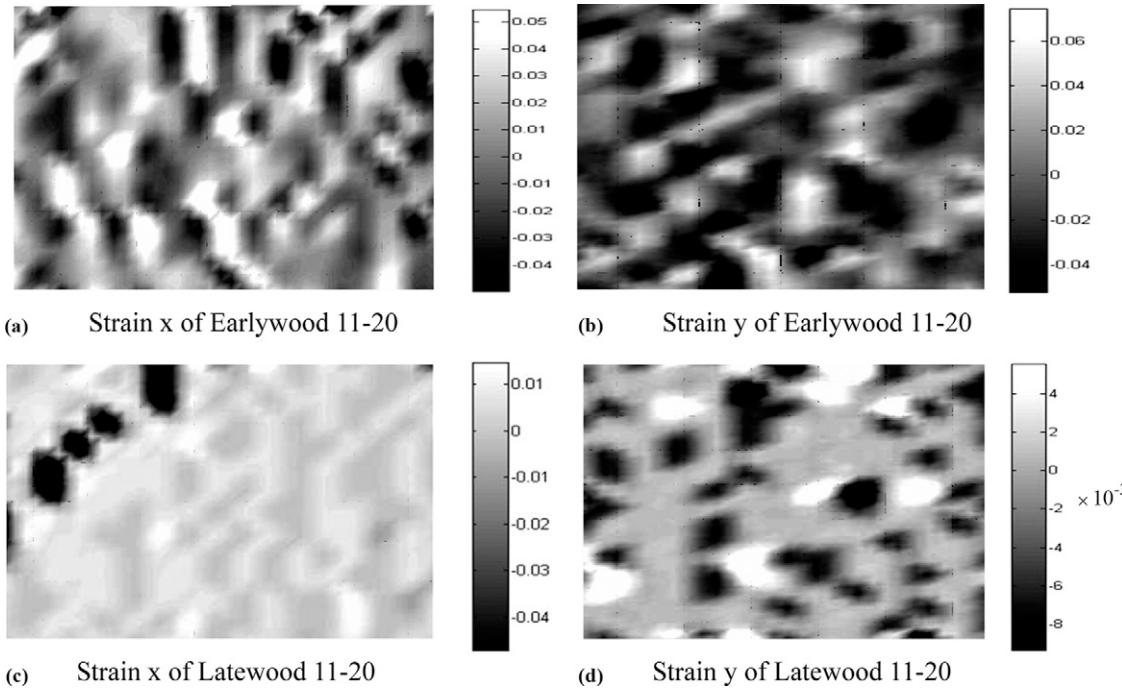

Figure 6. Strain distribution of earlywood and latewood from growth ring numbers 11 – 20 (specimen number 50 under 19.4 MPa and specimen number 50 under 19.8 MPa).

Figure 6 shows the strain distribution of specimen number 50 for the earlywood 11 – 20 and specimen number 50 for latewood 11 – 20. The magnitude of the strain distributions was much lower for earlywood and latewood from growth-ring numbers 11 – 20, which can be interpreted as a more oriented structure to the load direction for growth-ring numbers 11 – 20. Compared with growth-ring numbers 1 – 10, a higher MOE value for growth-ring numbers 11 – 20 can be seen from the strain distribution in x showing much lower magnitude in strain x of earlywood 11 – 20 and latewood 11 – 20. Under the same stress level, latewood 11 – 20 showed the most distinctive pattern for negative strain in x and negative strain in y from growth-ring numbers 11 – 20 resulted in the highest Poisson ratio among the groups.

Regardless of intraring layer and growth-ring positions, nonuniform strain distribution occurred in both directions during the testing. The average strain value used for the calculation of elastic modulus and Poisson ratio was in the 10^{-3} range; however, high oscillations of the strain distributions were observed on the cross-section. This is an interesting point that nonuniform strains occur in the middle of the cross-section away from the edge because uniform strain distribution within the gauge length is one of the assumptions made for ASTM D143 (ASTM 2004b) for tension and compression tests. However, from the results, the earlywood and latewood structures respond differently under a given load. Therefore, the elastic moduli of wood defined from ASTM D143 are actually effective moduli of the average of a set of individual fibers.

SUMMARY AND CONCLUSIONS

The physical and mechanical properties of earlywood and latewood from two different growth-ring positions showed different values.

The general trend was that specific gravity, MOE, UTS, and Poisson ratio generally increased with the increment of the growth-ring positions except for specific gravity and UTS from latewood. Although the MOE for earlywood and latewood was not dependent on the specific gravity, UTS for earlywood and latewood was highly dependent on specific gravity. From comparisons between current results and a previous study, MOE from earlywood and latewood showed a positive relationship with the height of the tree. Statistical comparisons showed that the MOE and UTS had a significant difference by both growth-ring and intraring positions. Distribution fitting showed that MOE for four groups were best fitted by Weibull distribution, whereas Poisson ratio was best fitted by Weibull distribution for earlywood 1 – 10 and latewood 11 – 20 groups and gamma distribution for earlywood 11 – 20 and latewood 1 – 10 groups. Strain distribution showed nonuniform distributions for four groups. Compared with earlywood 1 – 10 and latewood 1 – 10, earlywood 11 – 20 and latewood 11 – 20 showed more resistance to the load.

ACKNOWLEDGMENTS

This work was funded by the USDA National Research Initiative Competitive Grants Program (2005-35504-16115). Their financial contribution to this work is greatly acknowledged.

REFERENCES

ASTM (2004a) Standard test methods for specific gravity of wood and wood-based materials. D 2395-02. American Society for Testing and Materials, West Conshohocken, PA.

——— (2004b) Standard test methods for small clear specimens of timber. D 143-94. American Society for Testing and Materials, West Conshohocken, PA.

Bendtsen BA, Senft J (1986) Mechanical and anatomical properties in individual growth rings of plantation-grown Eastern cottonwood and loblolly pine. Wood Fiber Sci 18 (1):23 – 38.

Burdon RD, Kibblewhite RP, Walker JCF, Megraw RA, Evans R, Cown DJ (2004) Juvenile versus mature wood: a new concept, orthogonal to corewood versus outerwood, with special reference to *Pinus radiata* and *P. taeda*. Forest Sci 50(4):399 – 415.

Burgert I, Fruhmann K, Keckes J, Fratzl P, Stanzl-Tschegg SE (2003) Microtensile testing of wood fibers combined with video extensometry for efficient strain detection. Holzforschung 57:661 – 664.

Choi D, Thorpe JL, Hanna RB (1991) Image analysis to measure strain in wood and paper. Wood Sci Technol 25 (2):251 – 262.

Cramer SM, Kretschmann DE, Lakes R, Schmidt T (2005) Earlywood and latewood elastic properties in loblolly pine. Holzforschung 59(5):531 – 538.

Danvind J (2002) Methods for collecting and analysing simultaneous strain and moisture data during wood drying; Licenciate Thesis, Division of Wood Physics, Skelleftea Campus, Lulea University of Technology, Skelleftea, Sweden.

Eberl C, Thompson R, Gianola D (2006) Digital image correlation and tracking with Matlab. Matlab Central. http://www.mathworks.com/matlabcentral/fileexchange/loadFile.do?objectId=12413&objectType=FILE (27 September 2006).

Groom L, Mott L, Shaler S (2002) Mechanical properties of individual southern pine fibers. Part I. Determination and variability of stress-strain curves with respect to tree height and juvenility. Wood Fiber Sci 34 (1):14 – 27.

Hindman DP, Lee JN (2007) Modeling wood strands as multi-layer composites: Bending and tension loads. Wood Fiber Sci 39(4):515 – 526.

Jin H, Bruck HA (2005) Theoretical development for pointwise digital image correlation. Opt Eng 44(6): 1 – 14.

Keunecke D, Niemz P (2008) Axial stiffness and selected structural properties of yew and spruce microtensile specimens. Wood Res-Slovakia 53:1 – 14.

Kretschmann DE, Cramer SM, Lakes R, Schmidt T (2006) Selected mesostructure properties in loblolly pine from Arkansas plantations. Pages 149 – 170 *in* DD Stokke and LH Groom, eds. Characterization of the cellulosic cell wall. Blackwell, Oxford, UK.

Larson PR, Kretschmann DE, Clark A III, Isebrands JG (2001) Juvenile wood formation and properties in southern pine. Gen Tech Rep FPL-GTR-129. USDA Forest Prod Lab, Madison, WI.

Ljungdahl JL, Berglund A, Burman M (2006) Transverse anisotropy of compressive failure in European oak-a digital speckle photography study. Holzforschung 60 (2):190 – 195.

Mott L, Groom L, Shaler S (2002) Mechanical properties of individual southern pine fibers. Part II. Comparison of earlywood and latewood fibers with respect to tree height and juvenility. Wood Fiber Sci 34(2):221 – 237.

———, Shaler S, Groom L (1996) A novel technique to measure strain distributions in single wood fibers. Wood Fiber Sci 28(4):429 – 437.

Murata K, Masuda M (2001) Observation of microscopic swelling behavior of the cell wall. J Wood Sci 47 (6):507 – 509.

Muszynski L, Lopez-Anido R, Shaler S (2000) Image correlation analysis applied to measurement of shear strains in laminated composites. Pages 163 – 166 *in* Proc SEM IX International Congress on Experimental Mechanics, June 5 – 7, 2000, Orlando FL.

Penneru AP, Jayaramanand K, Bhattacharyya D (2005) Strain analysis in bulk forming of wood. Holzforschung 59(4):456 – 458.

Samarasinghe S, Kulasiri D (2004) Stress intensity factor of wood from crack-tip displacement fields obtained from digital image processing. Silva Fennica 38(3): 267 – 278.

SAS Institute Inc. (2004) SAS/STAT®, Version 9.1. Cary, NC.

Serrano E, Enquist B (2005) Contact-free measurement and non-linear finite element analyses of strain distribution along wood adhesive bonds. Holzforschung 59 (6):641 – 646.

Stelmokas JW, Zink AG, Loferski JL, Dolan JD (1997) Measurement of load distribution among multiple-bolted wood connections. J Test Eval 25(5):510 – 515.

Sun Y, Pang JHL, Wong CK, Su F (2005) Finite element formulation for a digital image correlation method. Appl Opt 44:7357 – 7363.

Taylor FW, Moore JS (1981) A comparison of earlywood and latewood tracheid lengths in loblolly pine. Wood Fiber Sci 13(3):159 – 165.

Xu P, Donaldson L, Walker J, Evans R, Downes G (2004) Effects of density and microfibril orientation on the vertical variation of low-stiffness wood in radiate pine butt logs. Holzforschung 58(6):673 – 677.

Yeh TF, Braun JL, Goldfarb B, Chang HM, Kadla JF (2006) Morphological and chemical variations between juvenile wood, mature wood, and compression wood of loblolly pine (*Pinus taeda* L.). Holzforschung 60 (1):1 – 8.

Zink AG, Davidson RW, Hanna RB (1995) Strain measurement in wood using a digital image correlation technique. Wood Fiber Sci 27(4):346 – 359.

Zink AG, Hanna RB, Stelmokas JW (1997) Measurement of Poisson's ratios for yellow-poplar. Forest Prod J 47 (3):78 – 80.